2010 IEEE International Conference on Robotics and Automation
Anchorage Convention District
May 3-8, 2010, Anchorage, Alaska, USA

Resonance-based Task Space Controller for Multi-Joint Robot with Adjustable Equilibrium Angle of Elastic Element

Mitsunori Uemura and Sadao Kawamura
Department of Robotics, Ritsumeikan University

***Abstract*— This paper proposes a task space trajectory tracking controller based on resonance for multi-joint robots. This controller generates desired motions, which are specified in the task space, while adjusting stiffness of mechanical elastic elements installed in each joint of the robots. This controller also adjusts equilibrium angles of the elastic elements. These parameter adjustments minimize actuator torque. Advantages of the proposed controller are to work without using exact parameter values of the controlled systems nor huge numerical calculations. We mathematically discuss stability of the controlled systems. Simulation results demonstrate the effectiveness of the proposed controller.**

***Index Terms*— Resonance, Task Space Control, Nonlinear Robot Dynamics, Stiffness Optimization**

I. INTRODUCTION

A. Conventional Resonance and Its Limitation

Resonance is one of the fundamental concepts for mechanical systems, and is utilized traditionally. If we utilize resonance, we can save energy while generating periodic motions. For example, pendulum clocks with limited energy sources are oscillated for long periods of time by using resonance.

However, conventional resonance has some limitations because conventional resonance is formulated only for sinusoidal motions of linear systems with one degree-of-freedom.

B. Resonance in Robotics

In the field of robotics, these limitations may have prevented researchers from utilizing resonance sufficiently, because multi-joint robots have nonlinear dynamics, multi degree-of-freedom, and requirements of non-sinusoidal motions.

Hitaka *et al.* tried to minimize driving energy of a flexible link robot in a hammering task [1]. In this case, however, even the robot has only one joint, to find optimal driving patterns could be done by only a numerical calculation or a reinforcement learning due to complex dynamics. Ozawa *et al.* proposed a adaptive motion controller with stiffness optimization [2]. The proposed controller is based on anti-resonance and can minimize energy consumption. However, anti-resonance is a concept for sinusoidal motions of linear systems. Therefore, the effectiveness of the proposed controller for multi-joint robots remained unclear. Control methods based on passive walking phenomena [3] also try to reduce energy consumption while generating periodic motions. However, the passive walking phenomena are completely passive motions, and may not be able to make clear how to utilize passive elements and actuators simultaneously.

C. Resonance-based Motion Control Method

To overcome these difficulties, we have proposed resonance-based motion control methods [4], [5], [6], [7]. These control methods can generate periodic motions of multi-joint robots while adaptively adjusting stiffness of mechanical elastic elements to minimize actuator torque [4]. If the desired motions are sinusoidal and dynamics is linear, the optimization concept of our control methods will be exactly the same as conventional resonance. Therefore, we could make clear that the proposed concept can be regarded as a kind of extension of conventional resonance.

On the other hand, we also proposed another type of a control method [5], [6], [7]. In this case, we adjust not only stiffness but also motion patterns. As a result, passive periodic motions, which require no actuator torque, could be generated in the case of multi-joint robots with no friction [5]. As a next step, we proposed an adaptation law of stiffness and motions to minimize actuator torque while generating periodic motions [6]. We tried to apply this controller to walking robots to generate energy saving walking motions [7].

Advantages of our control methods are to work well without using precise information of the controlled systems nor huge numerical calculations. Stability of some of these control methods are proved mathematically. Applications of the control methods are assumed to be human motion support systems [8], energy saving industrial robots and walking/running robots [7].

However, all of these previous controllers are designed in the joint space. In many robotic tasks, desired motions are specified in the task space. In addition, the previous controllers do not adjust equilibrium angles of the elastic elements, even the adjustment of the equilibrium angles may contribute further reduction of actuator torque.

D. Resonance-based Task Space Control

This paper tries to extend our controllers to task space, and design an adaptation law of equilibrium angles of elastic elements. Therefore, the desired motions in this paper are specified in the task space. We construct a task space controller with using a Jacobian matrix, even the elastic elements are adjusted in the joint space. The controller does not require calculations of inverse kinematics. We discuss stability of the controlled systems mathematically.

Additionally, this paper makes clear another important point that was unclear in our previous papers. Namely,

we analyze characteristics of the optimal stiffness, such as uniqueness and existence of local minimums.

II. Problem Formulation

A. Dynamics

Dynamics of multi-joint robots having n rotational joints with adjustable elastic elements as shown in **Fig.1** is described by

$$\boldsymbol{R}(\boldsymbol{q}(t))\ddot{\boldsymbol{q}}(t) + \left\{\frac{1}{2}\dot{\boldsymbol{R}}(\boldsymbol{q}(t)) + \boldsymbol{S}(\boldsymbol{q}(t), \dot{\boldsymbol{q}}(t)) + \boldsymbol{D}\right\}\dot{\boldsymbol{q}}(t) + \boldsymbol{g}(\boldsymbol{q}(t)) = -\boldsymbol{K}(t)(\boldsymbol{q}(t) - \boldsymbol{q_e}(t)) + \boldsymbol{\tau}(t), \quad (1)$$

where $\boldsymbol{R}(\boldsymbol{q}) \in \Re^{n\times n}$ is a positive definite inertia matrix, $\boldsymbol{S}(\boldsymbol{q}, \dot{\boldsymbol{q}}) \in \Re^{n\times n}$ is a skew symmetric matrix, $\boldsymbol{D} = \mathrm{diag}(d_1 \cdots d_n)$ is a viscosity matrix, $d_1 \cdots d_n \in \Re$ are coefficients of the viscosity, $\boldsymbol{g}(\boldsymbol{q}) \in \Re^n$ is a vector of gravitational torque, $\boldsymbol{K} = \mathrm{diag}(k_1 \cdots k_n)$ is a stiffness matrix, $k_1 \cdots k_n \in \Re$ are adjustable stiffness of the elastic elements installed in the each joint, $\boldsymbol{q} = (q_1 \cdots q_n)^T$ is a vector of joint angles, $\boldsymbol{q_e} = (q_{e1} \cdots q_{en})^T$ is a vector of equilibrium angles of the elastic elements, $\boldsymbol{\tau} = (\tau_1 \cdots \tau_2)^T$ is a vector of actuator torque, and t is time.

The stiffness $k_1 \cdots k_n$ are assumed to be adjustable in real-time. In addition to the adjustable stiffness, the equilibrium angles of the elastic elements $\boldsymbol{q_e}$ are also assumed to be adjustable in this paper. This point is different from our previous studies [4], [5]. When we use antagonistic elastic elements with nonlinear stiffness, we can adjust stiffness and equilibrium angles simultaneously. This kind of adjustable elastic elements has been developed by many researchers [9], [10], [11]. We also developed an adjustable elastic device, and confirmed that an actuator for the device does not consume much energy.

B. Characteristic of Dynamics

We use some characteristics of the robot dynamics in stability analysis, such as $\lambda_{max}(\boldsymbol{R}(\boldsymbol{q})) = e_1 > 0$, $\lambda_{min}(\boldsymbol{R}(\boldsymbol{q})) = e_2 > 0$, $||\boldsymbol{S}(\boldsymbol{q}, \dot{\boldsymbol{q}})|| < e_3||\dot{\boldsymbol{q}}||$, $\boldsymbol{g}(\boldsymbol{q})^T\boldsymbol{g}(\boldsymbol{q}) < e_4$, where $\lambda_{max}(\boldsymbol{R}(\boldsymbol{q})) \in \Re$ is a maximum eigenvalue of the matrix $\boldsymbol{R}(\boldsymbol{q})$, $\lambda_{min}(\boldsymbol{R}(\boldsymbol{q})) \in \Re$ is a minimum eigenvalue of the matrix $\boldsymbol{R}(\boldsymbol{q})$, $e_1, e_2, e_3, e_4 \in \Re$ are positive constants, and $||\boldsymbol{S}(\boldsymbol{q}, \dot{\boldsymbol{q}})|| \in \Re$ is square of the matrix norm of the matrix $\boldsymbol{S}(\boldsymbol{q}, \dot{\boldsymbol{q}})$ [12].

C. Kinematics

Kinematics of the robots can be described as $\boldsymbol{x} = \boldsymbol{f}(\boldsymbol{q}) \in \Re^n$. The dimension of the task space and joint space is assumed to be the same. Then, a Jacobian matrix $\boldsymbol{J}(\boldsymbol{q}) \in \Re^{n\times n}$ is defined as $\dot{\boldsymbol{x}} = \frac{\partial \boldsymbol{x}}{\partial \boldsymbol{q}}\dot{\boldsymbol{q}} = \boldsymbol{J}(\boldsymbol{q})\dot{\boldsymbol{q}}$.

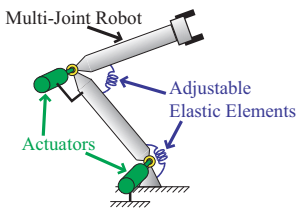

Fig. 1. Multi-Joint Robot with Adjustable Elastic Elements

D. Desired Motion

In this paper, we specify desired motions in the task space $\boldsymbol{x_d} = (x_{d1} \cdots x_{dn})^T \in \Re^n$. The desired motions are periodic $\boldsymbol{x_d}(t+T) = \boldsymbol{x_d}(t)$ with a cycle time T.

E. Assumption

In many cases, each component of the Jacobian matrix is finite, and the Jacobian matrix satisfies $||\boldsymbol{J}(\boldsymbol{q})|| < j_{max}$, where j_{max} is a positive constant. We assume that the robots will not always move close to neighborhood of singular points, and the minimum eigenvalue of the Jacobian matrix $\lambda_{min}(\boldsymbol{J}(\boldsymbol{q})) > j_{min}$ is a positive constant.

The desired motion $\boldsymbol{x_d}$ and its velocity $\dot{\boldsymbol{x}}_{\boldsymbol{d}}$ are assumed to be differentiable with respect to the time t and finite $|\boldsymbol{x_d}| < c_1$, $|\dot{\boldsymbol{x}}_{\boldsymbol{d}}| < c_2$, where $c_1, c_2 \in \Re$ are positive constants. The desired acceleration $\ddot{\boldsymbol{x}}_{\boldsymbol{d}}$ is also assumed to be finite $|\ddot{\boldsymbol{x}}_{\boldsymbol{d}}| < c_3$, where $c_3 \in \Re$ is a positive constant. Then, vector of desired angles $\boldsymbol{q_d} \in \Re^n$ and vector of desired angular velocities $\dot{\boldsymbol{q}}_{\boldsymbol{d}} \in \Re^n$ are calculated by $\boldsymbol{q_d} = \boldsymbol{f}^{-1}(\boldsymbol{x_d})$, $\dot{\boldsymbol{q}}_{\boldsymbol{d}} = \boldsymbol{J}(\boldsymbol{q})^{-1}\dot{\boldsymbol{x}}_{\boldsymbol{d}}$ respectively.

To avoid troublesome calculations of inverse kinematics, the desired angles $\boldsymbol{q_d}$ are assumed to be unavailable. On the other hand, we use the inverse matrix of the Jacobian matrix $\boldsymbol{J}(\boldsymbol{q})^{-1}$ to guarantee stability of the controlled systems. However, we also discuss another controller that does not require the inverse Jacobian matrix, and achieves control objectives. From the discussion of the kinematics in the section II-C and the above assumptions, $\boldsymbol{q_d}, \dot{\boldsymbol{q}}_{\boldsymbol{d}}, \ddot{\boldsymbol{q}}_{\boldsymbol{d}}$ become finite $|\boldsymbol{q_d}| < c_4$, $|\dot{\boldsymbol{q}}_{\boldsymbol{d}}| < c_5$, $|\ddot{\boldsymbol{q}}_{\boldsymbol{d}}| < c_6$, where $c_4, c_5, c_6 \in \Re$ are positive constants.

F. Control Objective

Under the above conditions, control objectives in this study are to generate the desired motion $\boldsymbol{x} \to \boldsymbol{x_d}$ by the actuator torque $\boldsymbol{\tau}$, and to minimize the actuator torque $\boldsymbol{\tau}$ by optimizing the stiffness $\boldsymbol{K}$ and the equilibrium angles $\boldsymbol{q_e}$.

III. Optimal Stiffness and Equilibrium Angle

In this section, we define the optimal stiffness $\boldsymbol{K_{opt}} = \mathrm{diag}(k_{opt1} \cdots k_{optn}) \in \Re^{n\times n}$ and equilibrium angles $\boldsymbol{q_{eopt}} = (q_{eopt1} \cdots q_{eoptn})^T \in \Re^n$ that minimizes the actuator torque $\boldsymbol{\tau}$. The optimal values $k_{opt1} \cdots k_{optn}, q_{eopt1} \cdots q_{eoptn}$ are assumed to be constants.

A. Necessary Torque for Generating Desired Motion

We can calculate the necessary actuator torque $\boldsymbol{\tau_d} \in \Re^n$, which is necessary to generate the desired motion, by substituting the desired motion $\boldsymbol{q_d}$, a constant stiffness matrix $\boldsymbol{K_s} = \mathrm{diag}(k_{s1} \cdots k_{sn})$ and a constant equilibrium angles $\boldsymbol{q_{es}} = (q_{es1} \cdots q_{esn})^T$ into $\boldsymbol{q}$, $\boldsymbol{K}(t)$ and $\boldsymbol{q_e}(t)$ of the dynamics (1) respectively.

$$\boldsymbol{\tau_d}(\boldsymbol{K_s}, \boldsymbol{q_{es}}, t) = \boldsymbol{R}(\boldsymbol{q_d})\ddot{\boldsymbol{q}}_{\boldsymbol{d}} + \left\{\frac{1}{2}\dot{\boldsymbol{R}}(\boldsymbol{q_d}) + \boldsymbol{S}(\boldsymbol{q_d}, \dot{\boldsymbol{q}}_{\boldsymbol{d}}) + \boldsymbol{D}\right\}\dot{\boldsymbol{q}}_{\boldsymbol{d}} + \boldsymbol{g}(\boldsymbol{q_d}) + \boldsymbol{K_s}(\boldsymbol{q_d} - \boldsymbol{q_{es}}) \quad (2)$$

B. Cost Function

Since our control objective is to minimize the actuator torque $\boldsymbol{\tau}$, we define the following cost function $J(\boldsymbol{K_s}, \boldsymbol{q_{es}})$ to be minimized.

$$J(\boldsymbol{K_s}, \boldsymbol{q_{es}}) = \int_{iT}^{iT+T} \boldsymbol{\tau_d}(\boldsymbol{K_s}, \boldsymbol{q_{es}}, t)^T \boldsymbol{\tau_d}(\boldsymbol{K_s}, \boldsymbol{q_{es}}, t)\mathrm{d}t, \quad (3)$$

where i is a counting number.

C. Definition of Optimal Stiffness and Equilibrium Angle

The optimal stiffness $\boldsymbol{K_{opt}}$ and equilibrium angles $\boldsymbol{q_{eopt}}$ are defined as the ones that minimize the cost function J. Then, $\boldsymbol{K_{opt}}$ and $\boldsymbol{q_{eopt}}$ satisfy the equation $J_{min} = J(\boldsymbol{K_{opt}}, \boldsymbol{q_{eopt}}) = \min_{\boldsymbol{K_s}, \boldsymbol{q_{es}}} J(\boldsymbol{K_s}, \boldsymbol{q_{es}})$, where J_{min} is the minimum of the cost function J. The optimal actuator torque is defined as $\boldsymbol{\tau_{dopt}}(t) = \boldsymbol{\tau_d}(\boldsymbol{K_{opt}}, \boldsymbol{q_{eopt}}, t)$.

D. Characteristics about Optimal Stiffness and Equilibrium Angle

We show some characteristics of the optimal stiffness $\boldsymbol{K_{opt}}$ and equilibrium angles $\boldsymbol{q_{eopt}}$. The stiffness values $k_{s1}, \cdots k_{sn}$ and the equilibrium angles $q_{es1} \cdots q_{esn}$ appear with the form of $k_{s1}(q_1 - q_{es1})$ in $\boldsymbol{\tau_d}$. Therefore, we can calculate pertial derivatives of $\boldsymbol{\tau_d}^T \boldsymbol{\tau_d}$ by them as $\frac{\partial(\boldsymbol{\tau_d}^T \boldsymbol{\tau_d})}{\partial k_{si}} = 2(q_{di} - q_{esi})\tau_{di}$, $\frac{\partial^2(\boldsymbol{\tau_d}^T \boldsymbol{\tau_d})}{\partial k_{si}^2} = 2(q_{di} - q_{esi})^2$, $\frac{\partial(\boldsymbol{\tau_d}^T \boldsymbol{\tau_d})}{\partial q_{esi}} = 2k_{si}\tau_{di}$, $\frac{\partial^2(\boldsymbol{\tau_d}^T \boldsymbol{\tau_d})}{\partial q_{esi}^2} = 2k_{si}^2$. Since we are assuming constant values of the stiffness and the equilibrium angles, $\frac{\partial^2 J}{\partial k_{si}^2} = 2\int_0^T (q_{di} - q_{esi})^2 dt = \mathrm{const}$ $\frac{\partial^2 J}{\partial q_{esi}^2} = 2\int_0^T k_{si}^2 dt = \mathrm{const}$ are satisfied. Therefore, J is a quadratic function of the stiffness values k_{si} and q_{esi}. This means that the optimal stiffness values and equilibrium angles are unique, and there are no local minimums.

IV. Controller

This section presents a task space controller, which is designed to realize the control objectives. This controller is composed of a stiffness adaptation and iterative learning control [12]. In general, the framework of the trajectory tracking for the periodic motions is called "repetitive control", but it is proved that iterative learning control also can treat this kind of framework [12]. The combination of these control methods brings about no requirement of the parameters of the controlled system nor huge numerical calculations.

Iterative learning control in this study has a special structure not to learn a certain torque pattern [4], which can be exerted by the torque of the elastic elements $\boldsymbol{Kq}$.

A. Design of Actuator Torque

We designed the actuator torque as

$$\boldsymbol{\tau}(t) = -\boldsymbol{J}(\boldsymbol{q})^T(\boldsymbol{K_v}\Delta\dot{\boldsymbol{x}} + \boldsymbol{K_p}\boldsymbol{s}(\Delta\boldsymbol{x})) + \boldsymbol{u}(t), \quad (4)$$

where $\boldsymbol{K_v} = \mathrm{diag}(k_{v1} \cdots k_{vn})$, $\boldsymbol{K_p} = \mathrm{diag}(k_{p1} \cdots k_{pn})$, $k_{v1} \cdots k_{vn} \in \Re$, $k_{p1} \cdots k_{pn} \in \Re$ are feedback gains, $\Delta\boldsymbol{x} = (\Delta x_1 \cdots \Delta x_n)^T = \boldsymbol{x} - \boldsymbol{x_d}$, $\boldsymbol{s}(\Delta\boldsymbol{x}) = (s_1(\Delta x_1) \cdots s_n(\Delta x_n))^T$, $\boldsymbol{u}(t) \in \Re^n$ is the feedfoward torque of learning control, and $s_1() \cdots s_n() \in \Re$ are saturated functions proposed by Arimoto *et al.* [12]. In this paper, we select the saturated functions as follows,

$$s_i(\Delta x_i) = \begin{cases} 1, & \Delta x_i > \frac{\pi}{2} \\ \sin(\Delta x_i), & \frac{\pi}{2} \geq \Delta x_i \geq -\frac{\pi}{2} \\ -1, & \Delta x_i < -\frac{\pi}{2} \end{cases} \quad (5)$$

It has been shown that the saturated function plays important roles to guarantee stability for the robot dynamics[12].

B. Adaptation of Stiffness and Equilibrium Angle

Since the stiffness matirx $\boldsymbol{K}(t)$ and the vector of the equilibrium angles $\boldsymbol{q_e}(t)$ appear as the bilinear form $\boldsymbol{K}(t)\boldsymbol{q_e}(t)$ in the dynamics (1), it is difficult to use usual parameter tuning structures of adaptive control for the bilinear term $\boldsymbol{K}(t)\boldsymbol{q_e}(t)$. Therefore, we consider the parameterization $\boldsymbol{K}(t)(\boldsymbol{q}(t) - \boldsymbol{q_c}) - \bar{\boldsymbol{q}}_{\boldsymbol{e}}(t) = \boldsymbol{K}(t)(\boldsymbol{q} - \boldsymbol{q_e}(t))$, where $\boldsymbol{q_c} = (q_{c1} \cdots q_{cn})^T$, $q_{c1} \cdots q_{cn}$ are constants, and $\bar{\boldsymbol{q}}_{\boldsymbol{e}} = \boldsymbol{K}(t)(\boldsymbol{q_e} - \boldsymbol{q_c})$. The actual equilibrium angles $\boldsymbol{q_e}$ should be adjusted by $q_{ei} = \frac{\bar{q}_{ei}}{k_i} + q_{ci}$. Under the above parameterization, the parameters $\boldsymbol{K}, \bar{\boldsymbol{q}}_{\boldsymbol{e}}$ are adjusted by the following law.

$$\dot{\boldsymbol{k}} = \boldsymbol{\Gamma_k}(\boldsymbol{Q} - \boldsymbol{Q_c})\boldsymbol{y} \quad (6)$$

$$\dot{\bar{\boldsymbol{q}}}_{\boldsymbol{e}} = -\boldsymbol{\Gamma_{qe}}\boldsymbol{y} \quad (7)$$

where $\boldsymbol{k} = (k_1 \cdots k_n)^T$, $\boldsymbol{Q} = \mathrm{diag}(q_1 \cdots q_n)$, $\boldsymbol{Q_c} = \mathrm{diag}(q_{c1} \cdots q_{cn})$ $\boldsymbol{\Gamma_k}, \boldsymbol{\Gamma_{qe}} \in \Re^{n \times n}$ are positive definite matrix of adaptive gains, and $\boldsymbol{y}(t) = (y_1 \cdots y_n)^T$ is defined as

$$\boldsymbol{y}(t) = \boldsymbol{J}(\boldsymbol{q})^{-1}(\Delta\dot{\boldsymbol{x}} + \alpha\boldsymbol{s}(\Delta\boldsymbol{x})), \quad (8)$$

where $\alpha \in \Re$ is a positive constant.

It is known that orthogonality of regressors in adaptive controllers contributes fast parameter convergences. If we could select $\boldsymbol{q_c}$ as the average value of the joint angle $\boldsymbol{q_c} = \frac{\int_0^t \boldsymbol{q}\mathrm{d}t}{t}$, orthogonality between the two regressors $\boldsymbol{Q} - \boldsymbol{Q_c}$, $\boldsymbol{I}$ will be satisfied $\int_0^t (\boldsymbol{Q} - \boldsymbol{Q_c})^T \boldsymbol{I}\mathrm{d}t = 0$. Therefore, to select appropriate $\boldsymbol{q_c}$ seems to be not difficult. Even if $\boldsymbol{q_c}$ is not appropriate, $\boldsymbol{q_c}$ will not affect stability.

The structure of the equations (6), (7) is similar to parameter adjustment laws of adaptive control.

We need to calculate the inverse matrix of Jacobian matrix $\boldsymbol{J}(\boldsymbol{q})^{-1}$ in the equation (8). To calculate the inverse matrix has some demerits, such as a high computational cost and singular point problems. On the other hand, we may be able to use $\boldsymbol{J}(\boldsymbol{q})^T$ instead of $\boldsymbol{J}(\boldsymbol{q})^{-1}$, because $\boldsymbol{J}(\boldsymbol{q})^T = (\boldsymbol{J}(\boldsymbol{q})^T\boldsymbol{J}(\boldsymbol{q}))\boldsymbol{J}(\boldsymbol{q})^{-1}$ seems to play similar roles to $\boldsymbol{J}(\boldsymbol{q})^{-1}$. However, it seems difficult to discuss stability in the case of the Jacobian transpose $\boldsymbol{J}(\boldsymbol{q})^T$. Therefore, we discuss stability in the case of the equation (8), and we investigate effectiveness of $\boldsymbol{J}(\boldsymbol{q})^T$ in numerical simulations.

C. Iterative Learning Control

The feedfoward torque of learning control $\boldsymbol{u}$ is designed by using the signals of the previous cycle.

$$\boldsymbol{u}(t) = \boldsymbol{u}(t - T) - \beta\boldsymbol{y}(t - T) - \boldsymbol{W}_i\bar{\boldsymbol{q}}(t - T), \quad (9)$$

where $\beta \in \Re$ is a learning gain, $\bar{\boldsymbol{q}} = (\bar{q}_1 \cdots \bar{q}_n)^T = \boldsymbol{q} - \boldsymbol{q_s}$, $\boldsymbol{q_s} = (q_{s1} \cdots q_{sn})^T$, $q_{s1} \cdots q_{sn}$ are positive constants,

$\boldsymbol{W}_i = \mathrm{diag}(w_{i1} \cdots w_{in})$, $w_{i1} \cdots w_{in} \in \Re$ are defined later. The feedfoward torque in the first cycle $\boldsymbol{u}(t)$ $(0 \leq t < T)$ is set to 0.

The structure of the learning update law of the equation (9) is different from usual learning controllers. This update law uses the special term $\boldsymbol{W}_i\bar{\boldsymbol{q}}(t-T)$ in addition to the term of the error signal $\boldsymbol{y}$. This special term is introduced by our previous paper [4] not to learn the certain torque pattern, which can be exerted by the elastic elements. We proved global stability of this type of update law with joint space controller mathematically.

Differently from our previous joint space controller [4], we can not use the signal of the desired joint angles $\boldsymbol{q_d}$ in this paper. Therefore, we use the actual angles $\boldsymbol{q}$ in stead of $\boldsymbol{q_d}$ in the equation (9). We can expect similar effects of $\boldsymbol{q}$ to $\boldsymbol{q_d}$, because we can rewrite $\boldsymbol{q}$ as $\boldsymbol{q} = \boldsymbol{q_d} + \Delta\boldsymbol{q}$, and $\Delta\boldsymbol{q}$ is an error feedback term, which is usually used in learning update laws.

The coefficients $w_{i1} \cdots w_{in}$ of the $i+1$th cycle ($iT \leq t < iT+T$) is updated at the begining of the $i+1$th cycle ($t = iT$) by using the signals of the ith cycle ($iT - T \leq t < iT$).

$$w_{ij} = \frac{\int_{iT-T}^{iT}(u_j - \beta y_j)\bar{q}_j \mathrm{d}t}{\int_{iT-T}^{iT}\bar{q}_j^2 \mathrm{d}t} \quad (j = 1, 2 \cdots n) \tag{10}$$

V. Stability Analysis

This section discusses stability of the controlled system with the proposed task space controller. Since some fundamental parts of stability analysis for combined controllers of the stiffness adaptation and iterative learning control are shown in our previous paper [4], we omit some of these parts due to space limitation.

A. Orthogonality of Some Signal

In this stability analysis, the following orthogonal relationships play important roles.

$$\int_{iT}^{iT+T}(\boldsymbol{u} - \beta\boldsymbol{y})^T\bar{\boldsymbol{q}}\mathrm{d}t = 0 \tag{11}$$

$$\int_{iT}^{iT+T}{\boldsymbol{\tau_{dopt}}}^T\bar{\boldsymbol{q}}_{\boldsymbol{d}}\mathrm{d}t = 0 \tag{12}$$

where $\bar{\boldsymbol{q}}_{\boldsymbol{d}} = \boldsymbol{q_d} - \boldsymbol{q_{eopt}}$.

Detail derivations of the equation (11), (12) are shown in our previous paper [4].

B. Error of Feedfoward Torque

Next, we consider the error of the feedfoward torque between $\boldsymbol{u}$ and $\boldsymbol{\tau_{dopt}}$. Therefore, we calculate the error $\Delta\boldsymbol{u}(t) = \boldsymbol{u}(t) - \boldsymbol{\tau_{dopt}}(t)$ by subtracting $\boldsymbol{\tau_{dopt}}$ from the both side of the equation (9).

$$\Delta\boldsymbol{u}(t+T) = \Delta\boldsymbol{u}(t) - \beta\boldsymbol{y}(t) - \boldsymbol{W}_i\bar{\boldsymbol{q}}(t) \tag{13}$$

Then, we can calculate L_2 norm of the both side of the equation (13) as

$$\begin{aligned} ||\Delta\boldsymbol{u}||_{L2}^{i+1,\boldsymbol{I}} &\leq ||\Delta\boldsymbol{u}||_{L2}^{i,\boldsymbol{I}} + 2\beta^2||\boldsymbol{y}||_{L2}^{i,\boldsymbol{I}} \\ &\quad -2\beta\int_{iT-T}^{iT}\Delta\boldsymbol{u}(t)^T\boldsymbol{y}(t)\mathrm{d}t \\ &\quad +2\int_{iT-T}^{iT}\boldsymbol{\tau_{dopt}}(t)^T\boldsymbol{W}_i\bar{\boldsymbol{q}}(t)\mathrm{d}t, \end{aligned} \tag{14}$$

where we defined the form of the norm $||\Delta\boldsymbol{u}||_{L2}^{i+1,\boldsymbol{I}}$ as $\int_{iT}^{(i+1)T}\Delta\boldsymbol{u}^T\boldsymbol{I}\Delta\boldsymbol{u}\mathrm{d}t$, and we used the equation (11), (12).

For this kind of the form of the equation (14), stability has been proved, if the following passivity of error dynamics [12] is satisfied.

$$\int_{iT-T}^{iT}\Delta\boldsymbol{u}(t)^T\boldsymbol{y}(t)\mathrm{d}t > V(iT) - V(iT-T) + c_7||\boldsymbol{y}||_{L2}^{i,\boldsymbol{I}}, \tag{15}$$

where $c_7 \in \Re$ is a positive constant.

C. Passivity of Error Dynamics

Here, we show the passivity of error dynamics (15). To do this, we define a scalar function V as

$$\begin{aligned} V(t) &= \Delta\dot{\boldsymbol{x}}^T\boldsymbol{R_J}(\boldsymbol{q})\Delta\dot{\boldsymbol{x}} + 2\sum_{i=1}^{n}(k_{pi} + \alpha k_{vi})p_{si}(\Delta x_i) \\ &\quad +2\alpha\Delta\dot{\boldsymbol{x}}^T\boldsymbol{R_J}(\boldsymbol{q})\boldsymbol{s}(\Delta\boldsymbol{x}) \\ &\quad +\Delta\boldsymbol{k}^T{\boldsymbol{\Gamma_k}}^{-1}\Delta\boldsymbol{k} + \boldsymbol{q_e}^T\boldsymbol{\Gamma_{qe}}\boldsymbol{q_e}, \end{aligned} \tag{16}$$

where $\boldsymbol{R_J}(\boldsymbol{q}) = \boldsymbol{J}(\boldsymbol{q})^{-T}\boldsymbol{R}(\boldsymbol{q})\boldsymbol{J}(\boldsymbol{q})^{-1}$, $\Delta\boldsymbol{q} = (\Delta q_1 \cdots \Delta q_n)^T = \boldsymbol{q} - \boldsymbol{q_d}$, $p_{s1}(), \cdots p_{sn}() \in \Re$ are potential functions, which satisfy $p_{sj}(\Delta x_j) = \int_0^{\Delta x_j} s_j(r)\mathrm{d}r$, $p_{sj}(0) = 0$ $(j = 1 \cdots n)$. This scalar function $V(t)$ will be always positive by setting enough large gains $\boldsymbol{K_v}, \boldsymbol{K_p}$.

Next, we calculate time derivative of $V(t)$ as

$$\begin{aligned} \dot{V}(t) &= -||\Delta\dot{\boldsymbol{x}}||^{\boldsymbol{K_v}+\boldsymbol{D}} - ||\boldsymbol{s}(\Delta\boldsymbol{x})||^{\alpha\boldsymbol{K_p}} \\ &\quad +\boldsymbol{y}^T(\boldsymbol{z} + \Delta\boldsymbol{u}) + z_c \end{aligned} \tag{17}$$

$$\begin{aligned} \boldsymbol{z} &= -\left\{\boldsymbol{R}(\boldsymbol{q}) - \boldsymbol{R}(\boldsymbol{q_d})\right\}\ddot{\boldsymbol{q}}_{\boldsymbol{d}} - \frac{1}{2}\left\{\dot{\boldsymbol{R}}(\boldsymbol{q}) - \dot{\boldsymbol{R}}(\boldsymbol{q_d})\right\}\dot{\boldsymbol{q}}_{\boldsymbol{d}} \\ &\quad -\boldsymbol{S}(\boldsymbol{q}, \dot{\boldsymbol{q}})\dot{\boldsymbol{q}} + \boldsymbol{S}(\boldsymbol{q_d}, \dot{\boldsymbol{q}}_{\boldsymbol{d}})\dot{\boldsymbol{q}}_{\boldsymbol{d}} - \boldsymbol{g}(\boldsymbol{q}) + \boldsymbol{g}(\boldsymbol{q_d}). \end{aligned} \tag{18}$$

$$\begin{aligned} z_c &= \boldsymbol{y}^T\boldsymbol{R}(\boldsymbol{q})(\ddot{\boldsymbol{q}}_{\boldsymbol{d}} - \boldsymbol{J}(\boldsymbol{q})^{-1}\ddot{\boldsymbol{x}}_{\boldsymbol{d}}) \\ &\quad +\boldsymbol{y}^T\boldsymbol{D}(\dot{\boldsymbol{q}}_{\boldsymbol{d}} - \boldsymbol{J}(\boldsymbol{q})^{-1}\dot{\boldsymbol{x}}_{\boldsymbol{d}}) - \boldsymbol{y}^T\boldsymbol{K_{opt}}\Delta\boldsymbol{q} \\ &\quad +\alpha\Delta\dot{\boldsymbol{x}}^T\dot{\boldsymbol{R}}_{\boldsymbol{J}}(\boldsymbol{q})\boldsymbol{s}(\Delta\boldsymbol{x}) + \alpha\Delta\dot{\boldsymbol{x}}^T\boldsymbol{R_J}(\boldsymbol{q})\dot{\boldsymbol{s}}(\Delta\boldsymbol{x}) \end{aligned} \tag{19}$$

where we define the form of the norm $||\Delta\dot{\boldsymbol{x}}||^{\boldsymbol{K_v}+\boldsymbol{D}}$ as $\Delta\dot{\boldsymbol{x}}^T(\boldsymbol{K_v} + \boldsymbol{D})\Delta\dot{\boldsymbol{x}}$. By using the characteristic of the robot dynamics, the saturated functions, the Jacobian matrix, and the assumptions of the section II-E, the terms $\boldsymbol{y}^T\boldsymbol{z} + z_c$ of the right-hand side of the equation (17) satisfies the following inequality [12].

$$\boldsymbol{y}^T\boldsymbol{z} + z_c < c_8||\Delta\dot{\boldsymbol{x}}||^{\boldsymbol{I}} + c_9||\boldsymbol{s}(\Delta\boldsymbol{x})||^{\boldsymbol{I}} \tag{20}$$

where $c_8, c_9 \in \Re$ are positive constants.

The constants c_8, c_9 are independent of the feedback gains $\boldsymbol{K_v}, \boldsymbol{K_p}$. Therefore, we can select a positive constant c_7,

which satisfies the following inequality, from the equations (17), (20) by setting enough large gains $\boldsymbol{K_v}, \boldsymbol{K_p}$.

$$\dot{V}(t) \quad < \quad -c_7||\boldsymbol{y}||^{\boldsymbol{I}} + \boldsymbol{y}^T \Delta \boldsymbol{u} \tag{21}$$

By integrating the equation (21) by time t from iT to $iT+T$, we obtain the passivity of the error dynamics (15).

D. Convergence Analysis

Based on the above discussion, we discuss convergence of the state variables $\boldsymbol{q}, \dot{\boldsymbol{q}}$, and the parameters $\boldsymbol{K}, \boldsymbol{q_e}$.

First, we define a positive scalar function N_i of the ith cycle.

$$N_i = ||\Delta \boldsymbol{u}||^{i,\boldsymbol{I}}_{L2} + V(iT) \tag{22}$$

Next, by substituting the equations (22) and (15) into (14), we obtain

$$\begin{aligned} N_{i+1} \quad < \quad & N_i - (2\beta^2 - 2\beta c_7)||\boldsymbol{y}||^{\boldsymbol{I}}_{L2} \\ & +2\int_{iT-T}^{iT} \boldsymbol{\tau_{dopt}}(t)^T \boldsymbol{W}_i \bar{\boldsymbol{q}}(t) \mathrm{d}t. \end{aligned} \tag{23}$$

If we ignore the third term of the equation (23), the function N_i decreases in every cycle by setting enough small β or enough large c_7 by setting large gains $\boldsymbol{K_v}, \boldsymbol{K_p}$, This third term $\int_{iT-T}^{iT} \boldsymbol{\tau_{dopt}}(t)^T \boldsymbol{W}_i \bar{\boldsymbol{q}}(t) \mathrm{d}t$ can be rewritten by using the orthogonality of the equation (12) as $\int_{iT-T}^{iT} \boldsymbol{\tau_{dopt}}^T \boldsymbol{W}_i \Delta \boldsymbol{q}(t) \mathrm{d}t$. Then, this term will decrease with decrease of $\Delta \boldsymbol{q}(t)$. Therefore, around neighborhood of $\Delta \boldsymbol{q} = 0$, the decrease of N_i will be guaranteed.

Then, the N_i will converge to constant, and the L_2 norm of $\boldsymbol{y}$ will converge to 0. Then, we can guarantee $\dot{\boldsymbol{x}} \to \dot{\boldsymbol{x}}_{\boldsymbol{d}}$, $\boldsymbol{x} \to \boldsymbol{x_d}$ as $t \to \infty$ in the sense of L_2 norm.

The convergence of $\dot{\boldsymbol{x}} \to \dot{\boldsymbol{x}}_{\boldsymbol{d}}$, $\boldsymbol{x} \to \boldsymbol{x_d}$ guarantees convergence of the stiffness $\boldsymbol{K} \to \boldsymbol{K_{opt}}$, the equilibrium angles $\bar{\boldsymbol{q}}_{\boldsymbol{e}} \to \boldsymbol{K_{opt}} \boldsymbol{q_{eopt}}$, and the actuator torque $\boldsymbol{\tau} \to \boldsymbol{\tau_{dopt}}$ [4].

Therefore, we proved the stability of the control system with the proposed controller around neighborhood of $\Delta \boldsymbol{q} = 0$. To prove stability in the more global sense is our important future work.

VI. Simulation

We conducted numerical simulations to show the effectiveness of the proposed controller. We used a two joint planar robot as a simulation model as shown in **Fig.2**.

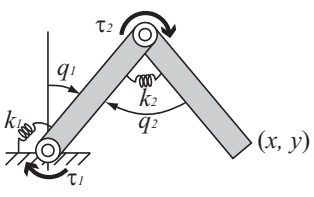

Fig. 2. Simulation Model

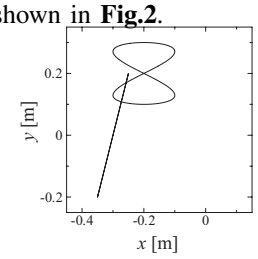

Fig. 3. Desired Motion in Cartesian Space

A. Condition

We adopted the equation (1) as dynamics of the simulation model. Each parameter of the robot was set to $m_1 = 3.0$[kg], $m_2 = 2.0$[kg], $l_1 = 0.3$[m], $l_2 = 0.25$[m], $l_{g1} = 0.13$[m], $l_{g2} = 0.1$[m], $I_1 = 0.01$[Nms^2/rad], $I_2 = 0.005$[Nms^2/rad], $d_1 = 0.2$[Nms/rad], $d_2 = 0.1$[Nms/rad], $k_1(0) = 0.0$[Nm/rad], $k_2(0) = 0.0$[Nm/rad], $q_{e1}(0) = 0.0$[rad], and $q_{e2}(0) = 0.0$[rad], where m is a weight of the robot link, l is a length of the link, l_g is a length from a joint to a mass center of the link, I is an inertia moment around the mass center of the link, and the number of the suffix j represents jth link.

The equations from (4) to (10) were adopted as a controller of the simulation. The gains were set to $k_{v1} = 200$[Ns/m], $k_{v2} = 200$[Ns/m], $k_{p1} = 2000$[N/m], $k_{p2} = 2000$[N/m], $\alpha = 10$, $\gamma_{k1} = 50$, $\gamma_{k2} = 5$, $\gamma_{qe1} = 150$, $\gamma_{qe2} = 10$, $\beta = 1$.

The tip position $\boldsymbol{x}$ is described as $\boldsymbol{x} = (x, y)^T$, $x = l_1 \cos(q_1) + l_2 \cos(q_1 + q_2)$, $y = l_1 \sin(q_1) + l_2 \sin(q_1 + q_2)$. The desired motion $\boldsymbol{x_d} = (x_d, y_d)^T$ is designed in the task space as $x_d = 0.05 \sin(2\pi t) - 0.3$[m], $y_d = -0.2 \sin(2\pi t)$[m] in first 40 seconds $0 \le t < 40$[s], and $x_d = 0.1 \sin(2\pi t) - 0.2$[m], $y_d = 0.1 \cos(4\pi t) + 0.2$[m] in the next 40 seconds $40 \le t < 80$[s] as shown in **Fig.3**.

B. Result

We obtained simulation results as shown in **Fig.4**. The tip position x, y converged to the desired ones x_d, y_d as shown in **Fig.4(a)**, **(b)**. The stiffness k_1, k_2 almost converged to the optimal ones k_{opt1}, k_{opt2} as shown in **Fig.4(c)**, **(d)**. The parameters of the equilibrium angles $\bar{q}_{e1}, \bar{q}_{e2}$ almost converged to the optimal ones $\bar{q}_{eopt1}, \bar{q}_{eopt2}$ as shown in **Fig.4(e)**, **(f)**. We calculated these optimal values $k_{opt1}, k_{opt2}, \bar{q}_{eopt1}, \bar{q}_{eopt2}$ by using a numerical method. The convergences of the parameters were slower and less precise than our previous simulation results [4]. The reason of the worse convergences seems that the number of the parameters in the proposed adaptive law is greater than our previous adaptive law. Increase of the number of parameters in adaptive control usually worsen parameter convergences. Even the worse parameter convergences, the actuator torque τ_1, τ_2 converged to the optimal ones $\tau_{dopt1}, \tau_{dopt2}$ not so slower nor less precise as shown in **Fig.4(g)**, **(h)**. The amount of the converged actuator torque $\int_{t_1}^{t_2} \boldsymbol{\tau}(t)^T \boldsymbol{\tau}(t) \mathrm{d}t$ in $t_1 = 39, t_2 = 40$[s] was about 98[%] smaller than the case without the stiffness and equilibrium angle adjustments $\int_{t_1}^{t_2} \boldsymbol{\tau_d}(0,0,t)^T \boldsymbol{\tau_d}(0,0,t) \mathrm{d}t$. The reduction ratio in the case of $t_1 = 79, t_2 = 80$[s] was 84[%].

C. Discussion

Even the stability analysis in the section V is not global, the simulation results demonstrated that the proposed controller can reduce actuator torque significantly by the stiffness and equilibrium angle adaptation.

Moreover, we conducted another simulation to verify whether the inverse Jacobian matrix $\boldsymbol{J}(\boldsymbol{q})^{-1}$ in the equation (8) can be replaced by the transpose of it $\boldsymbol{J}(\boldsymbol{q})^T$ or not. This replacement enables to avoid troublesome calculations of the

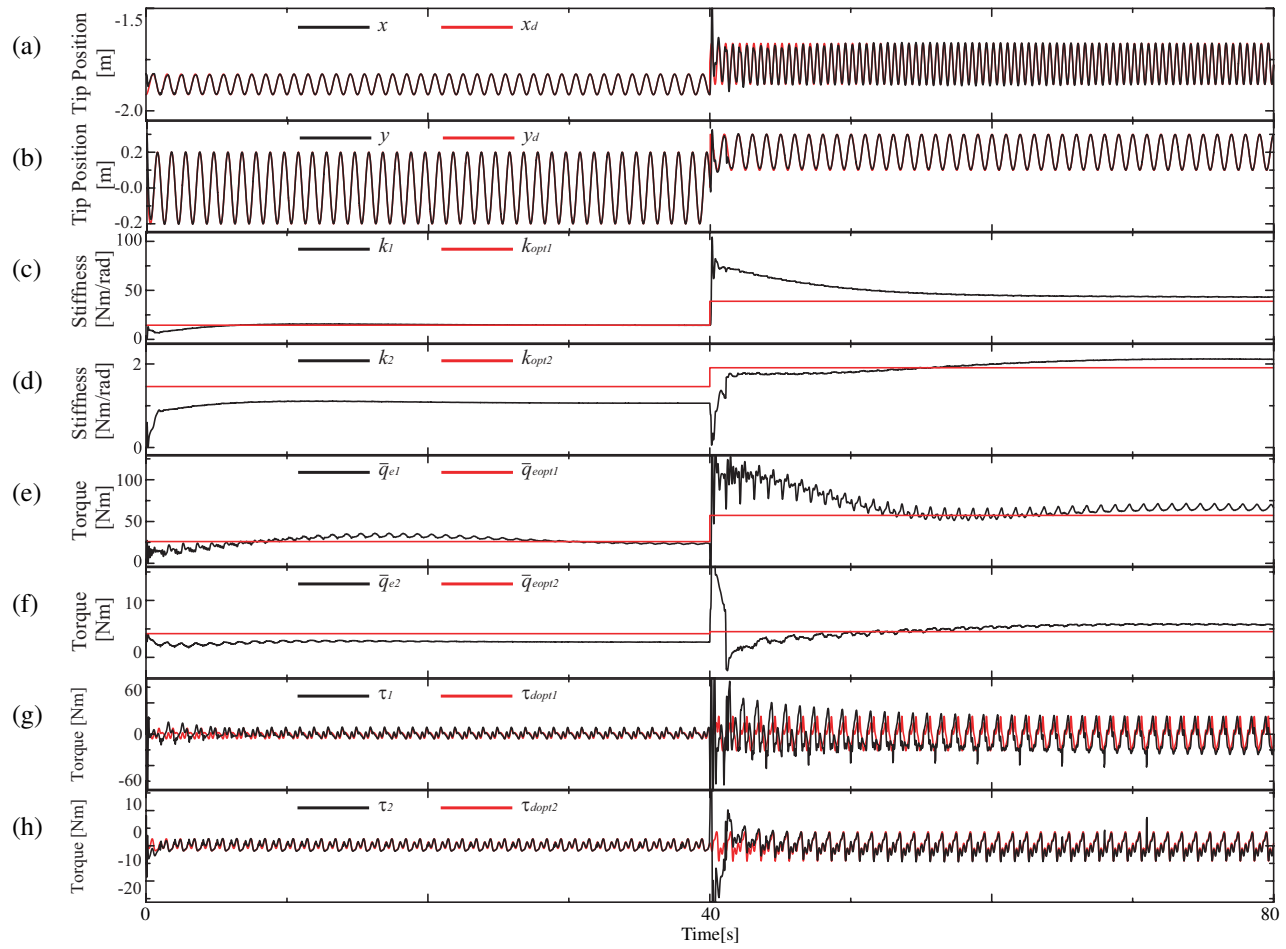

Fig. 4. Simulation Results

inverse matrix. Even in the case of the transpose matrix, we could obtain almost the same results. In the future, we will try to prove stability of the controlled systems with the controller of the Jacobian transpose matrix.

VII. Conclusion

This paper has proposed a resonance-based task space controller for multi-joint robots with an equilibrium angle adjustment. The proposed controller adjusts not only stiffness but also equilibrium angles of mechanical elastic elements. Then, actuator torque will be reduced as much as possible. Advantages of the proposed controller is not to use exact parameter values of the controlled systems nor huge numerical calculations. Stability of the controlled systems with the proposed controller was discussed in detail. The effectiveness of the proposed controller was verified thorough simulation results.

To prove more global stability is one of our important future works.

References

[1] Y. Hitaka, T. Izumi: "Minimum Energy Driving of a Flexible Link Hammer Using Neural Networks," *IROS1995*, vol. 3, pp. 320-325, 1995.
[2] R. Ozawa, H. Kobayashi: "A new impedance control concept for elastic joint robots," *ICRA2003*, vol. 3, pp. 3126-3131, 2003.
[3] T. McGeer, "Passive Dynamic Walking", *Robotics Research*, Vol. 9, No. 2, pp. 62-82, 1990.
[4] M. Uemura, S. Kawamura: "Resonance-based Motion Control Method for Multi-Joint Robot through Combining Stiffness Adaptation and Iterative Learning Control", *ICRA2009*, pp. 1543-1548, 2009.
[5] M. Uemura, G. Lu, S. Kawamura, S. Ma: "Passive Periodic Motions of Multi-Joint Robots by Stiffness Adaptation and DFC for Energy Saving", *SICE2008*, pp. 2853-2858, 2008.
[6] M. Uemura, S. Kawamura: "Generation of Energy Saving Motion for Biped Walking Robot through Resonance-based Control Method", *SYROCO2009*, pp. 607-612, 2009.
[7] M. Uemura, K. Kimura, S. Kawamura: "Generation of Energy Saving Motion for Biped Walking Robot through Resonance-based Control Method", *IROS2009*, pp. 2928-2933, 2009.
[8] M. Uemura, K. Kanaoka, S. Kawamura: "Power Assist System for Sinusoidal Motion by Passive Element and Impedance Control", *ICRA2006*, pp. 3935-3940, 2006.
[9] T. Morita, S. Sugano: "Development of 4-D.O.F Manipulator Using Mechanical Impedance Adjuster", *ICRA1996*, Vol. 4, pp. 2902-2907, 1996.
[10] K. Koganezawa: "Mechanical Stiffness Control for Antagonistically Driven Joints", *IROS2005*, pp. 1544-1551, 2005.
[11] H. Noborisaka, H. Kokayashi: "Design of a Tendon-Driven Articulated Finger-Hand Mechanism and Its Stiffness Adjustability", *JSME International Journal. Series C, Mechanical Systems, Machine Elements and Manufacturing*, Vol. 43, No. 3, pp. 638-644, 2000.
[12] S. Arimoto: Control Theory of Non-Linear Mechanical Systems: A Passivity-Based and Circuit-Theoretic Approach. *Oxford Engineering Science Series*, 1996.